Observation of the electromagnetic Dalitz decay $D^{*0} \to D^0 e^+ e^-$

M. Ablikim,[1] M. N. Achasov,[10,b] P. Adlarson,[66] S. Ahmed,[14] M. Albrecht,[4] R. Aliberti,[27] A. Amoroso,[65a,65c] M. R. An,[31] Q. An,[62,48] X. H. Bai,[56] Y. Bai,[47] O. Bakina,[28] R. Baldini Ferroli,[22a] I. Balossino,[23a] Y. Ban,[37,h] K. Begzsuren,[25] N. Berger,[27] M. Bertani,[22a] D. Bettoni,[23a] F. Bianchi,[65a,65c] J. Bloms,[59] A. Bortone,[65a,65c] I. Boyko,[28] R. A. Briere,[5] H. Cai,[67] X. Cai,[1,48] A. Calcaterra,[22a] G. F. Cao,[1,53] N. Cao,[1,53] S. A. Cetin,[52a] J. F. Chang,[1,48] W. L. Chang,[1,53] G. Chelkov,[28,a] D. Y. Chen,[6] G. Chen,[1] H. S. Chen,[1,53] M. L. Chen,[1,48] S. J. Chen,[34] X. R. Chen,[24] Y. B. Chen,[1,48] Z. J. Chen,[19,i] W. S. Cheng,[65c] G. Cibinetto,[23a] F. Cossio,[65c] X. F. Cui,[35] H. L. Dai,[1,48] X. C. Dai,[1,53] A. Dbeyssi,[14] R. E. de Boer,[4] D. Dedovich,[28] Z. Y. Deng,[1] A. Denig,[27] I. Denysenko,[28] M. Destefanis,[65a,65c] F. De Mori,[65a,65c] Y. Ding,[32] C. Dong,[35] J. Dong,[1,48] L. Y. Dong,[1,53] M. Y. Dong,[1,48,53] X. Dong,[67] S. X. Du,[70] Y. L. Fan,[67] J. Fang,[1,48] S. S. Fang,[1,53] Y. Fang,[1] R. Farinelli,[23a] L. Fava,[65b,65c] F. Feldbauer,[4] G. Felici,[22a] C. Q. Feng,[62,48] J. H. Feng,[49] M. Fritsch,[4] C. D. Fu,[1] Y. Gao,[37,h] Y. Gao,[62,48] Y. G. Gao,[6] I. Garzia,[23a,23b] P. T. Ge,[67] C. Geng,[49] E. M. Gersabeck,[57] A. Gilman,[60] K. Goetzen,[11] L. Gong,[32] W. X. Gong,[1,48] W. Gradl,[27] M. Greco,[65a,65c] L. M. Gu,[34] M. H. Gu,[1,48] C. Y. Guan,[1,53] A. Q. Guo,[21] L. B. Guo,[33] R. P. Guo,[39] Y. P. Guo,[9,f] A. Guskov,[28,a] T. T. Han,[40] W. Y. Han,[31] X. Q. Hao,[15] F. A. Harris,[55] K. L. He,[1,53] F. H. Heinsius,[4] C. H. Heinz,[27] Y. K. Heng,[1,48,53] C. Herold,[50] M. Himmelreich,[11,d] T. Holtmann,[4] G. Y. Hou,[1,53] Y. R. Hou,[53] Z. L. Hou,[1] H. M. Hu,[1,53] J. F. Hu,[46,j] T. Hu,[1,48,53] Y. Hu,[1] G. S. Huang,[62,48] L. Q. Huang,[63] X. T. Huang,[40] Y. P. Huang,[1] Z. Huang,[37,h] T. Hussain,[64] N. Hüsken,[21,27] W. Ikegami Andersson,[66] W. Imoehl,[21] M. Irshad,[62,48] S. Jaeger,[4] S. Janchiv,[25] Q. Ji,[1] Q. P. Ji,[15] X. B. Ji,[1,53] X. L. Ji,[1,48] Y. Y. Ji,[40] H. B. Jiang,[40] X. S. Jiang,[1,48,53] J. B. Jiao,[40] Z. Jiao,[17] S. Jin,[34] Y. Jin,[56] M. Q. Jing,[1,53] T. Johansson,[66] N. Kalantar-Nayestanaki,[54] X. S. Kang,[32] R. Kappert,[54] M. Kavatsyuk,[54] B. C. Ke,[42,1] I. K. Keshk,[4] A. Khoukaz,[59] P. Kiese,[27] R. Kiuchi,[1] R. Kliemt,[11] L. Koch,[29] O. B. Kolcu,[52a,m] B. Kopf,[4] M. Kuemmel,[4] M. Kuessner,[4] A. Kupsc,[66] M. G. Kurth,[1,53] W. Kühn,[29] J. J. Lane,[57] J. S. Lange,[29] P. Larin,[14] A. Lavania,[20] L. Lavezzi,[65a,65c] Z. H. Lei,[62,48] H. Leithoff,[27] M. Lellmann,[27] T. Lenz,[27] C. Li,[38] C. H. Li,[31] Cheng Li,[62,48] D. M. Li,[70] F. Li,[1,48] G. Li,[1] H. Li,[62,48] H. Li,[42] H. B. Li,[1,53] H. J. Li,[15] H. N. Li,[46,j] J. L. Li,[40] J. Q. Li,[4] J. S. Li,[49] Ke Li,[1] L. K. Li,[1] Lei Li,[3] P. R. Li,[30,k,l] S. Y. Li,[51] W. D. Li,[1,53] W. G. Li,[1] X. H. Li,[62,48] X. L. Li,[40] Xiaoyu Li,[1,53] Z. Y. Li,[49] H. Liang,[62,48] H. Liang,[1,53] H. Liang,[26] Y. F. Liang,[44] Y. T. Liang,[24] G. R. Liao,[12] L. Z. Liao,[1,53] J. Libby,[20] C. X. Lin,[49] T. Lin,[1] B. J. Liu,[1] C. X. Liu,[1] D. Liu,[14,62] F. H. Liu,[43] Fang Liu,[1] Feng Liu,[6] G. M. Liu,[46,j] H. M. Liu,[1,53] Huanhuan Liu,[1] Huihui Liu,[16] J. B. Liu,[62,48] J. L. Liu,[63] J. Y. Liu,[1,53] K. Liu,[1] K. Y. Liu,[32] L. Liu,[62,48] M. H. Liu,[9,f] P. L. Liu,[1] Q. Liu,[67] Q. Liu,[53] S. B. Liu,[62,48] T. Liu,[1,53] W. M. Liu,[62,48] X. Liu,[30,k,l] Y. Liu,[30,k,l] Y. B. Liu,[35] Z. A. Liu,[1,48,53] Z. Q. Liu,[40] X. C. Lou,[1,48,53] F. X. Lu,[49] H. J. Lu,[17] J. D. Lu,[1,53] J. G. Lu,[1,48] X. L. Lu,[1] Y. Lu,[1] Y. P. Lu,[1,48] C. L. Luo,[33] M. X. Luo,[69] P. W. Luo,[49] T. Luo,[9,f] X. L. Luo,[1,48] X. R. Lyu,[53] F. C. Ma,[32] H. L. Ma,[1] L. L. Ma,[40] M. M. Ma,[1,53] Q. M. Ma,[1] R. Q. Ma,[1,53] R. T. Ma,[53] X. X. Ma,[1,53] X. Y. Ma,[1,48] F. E. Maas,[14] M. Maggiora,[65a,65c] S. Maldaner,[4] S. Malde,[60] Q. A. Malik,[64] A. Mangoni,[22b] Y. J. Mao,[37,h] Z. P. Mao,[1] S. Marcello,[65a,65c] Z. X. Meng,[56] J. G. Messchendorp,[54] G. Mezzadri,[23a] T. J. Min,[34] R. E. Mitchell,[21] X. H. Mo,[1,48,53] N. Yu. Muchnoi,[10,b] H. Muramatsu,[58] S. Nakhoul,[11,d] Y. Nefedov,[28] F. Nerling,[11,d] I. B. Nikolaev,[10,b] Z. Ning,[1,48] S. Nisar,[8,g] S. L. Olsen,[53] Q. Ouyang,[1,48,53] S. Pacetti,[22b,22c] X. Pan,[9,f] Y. Pan,[57] A. Pathak,[1] A. Pathak,[26] P. Patteri,[22a] M. Pelizaeus,[4] H. P. Peng,[62,48] K. Peters,[11,d] J. Pettersson,[66] J. L. Ping,[33] R. G. Ping,[1,53] S. Pogodin,[28] R. Poling,[58] V. Prasad,[62,48] H. Qi,[62,48] H. R. Qi,[51] M. Qi,[34] T. Y. Qi,[9] S. Qian,[1,48] W. B. Qian,[53] Z. Qian,[49] C. F. Qiao,[53] J. J. Qin,[63] L. Q. Qin,[12] X. P. Qin,[9] X. S. Qin,[40] Z. H. Qin,[1,48] J. F. Qiu,[1] S. Q. Qu,[35] K. H. Rashid,[64] K. Ravindran,[20] C. F. Redmer,[27] A. Rivetti,[65c] V. Rodin,[54] M. Rolo,[65c] G. Rong,[1,53] Ch. Rosner,[14] M. Rump,[59] H. S. Sang,[62] A. Sarantsev,[28,c] Y. Schelhaas,[27] C. Schnier,[4] K. Schoenning,[66] M. Scodeggio,[23a,23b] W. Shan,[18] X. Y. Shan,[62,48] J. F. Shangguan,[45] M. Shao,[62,48] C. P. Shen,[9] H. F. Shen,[1,53] X. Y. Shen,[1,53] H. C. Shi,[62,48] R. S. Shi,[1,53] X. Shi,[1,48] X. D. Shi,[62,48] J. J. Song,[40] W. M. Song,[26,1] Y. X. Song,[37,h] S. Sosio,[65a,65c] S. Spataro,[65a,65c] K. X. Su,[67] P. P. Su,[45] F. F. Sui,[40] G. X. Sun,[1] H. K. Sun,[1] J. F. Sun,[15] L. Sun,[67] S. S. Sun,[1,53] T. Sun,[1,53] W. Y. Sun,[26] X. Sun,[19,i] Y. J. Sun,[62,48] Y. Z. Sun,[1] Z. T. Sun,[1] Y. H. Tan,[67] Y. X. Tan,[62,48] C. J. Tang,[44] G. Y. Tang,[1] J. Tang,[49] J. X. Teng,[62,48] V. Thoren,[66] W. H. Tian,[42] Y. T. Tian,[24] I. Uman,[52b] B. Wang,[1] C. W. Wang,[34] D. Y. Wang,[37,h] H. J. Wang,[30,k,l] H. P. Wang,[1,53] K. Wang,[1,48] L. L. Wang,[1] M. Wang,[40] M. Z. Wang,[37,h] Meng Wang,[1,53] S. Wang,[9,f] W. Wang,[49] W. H. Wang,[67] W. P. Wang,[62,48] X. Wang,[37,h] X. F. Wang,[30,k,l] X. L. Wang,[9,f] Y. Wang,[49] Y. D. Wang,[36] Y. F. Wang,[1,48,53] Y. Q. Wang,[1] Y. Y. Wang,[30,k,l] Z. Wang,[1,48] Z. Y. Wang,[1] Ziyi Wang,[53] Zongyuan Wang,[1,53] D. H. Wei,[12] F. Weidner,[59] S. P. Wen,[1] D. J. White,[57] U. Wiedner,[4] G. Wilkinson,[60] M. Wolke,[66] L. Wollenberg,[4] J. F. Wu,[1,53] L. H. Wu,[1] L. J. Wu,[1,53] X. Wu,[9,f] X. H. Wu,[26] Z. Wu,[1,48] L. Xia,[62,48] H. Xiao,[9,f] S. Y. Xiao,[1] Z. J. Xiao,[33] X. H. Xie,[37,h] Y. G. Xie,[1,48] Y. H. Xie,[6] T. Y. Xing,[1,53] G. F. Xu,[1] Q. J. Xu,[13] W. Xu,[1,53] X. P. Xu,[45] Y. C. Xu,[53] F. Yan,[9,f] L. Yan,[9,f] W. B. Yan,[62,48] W. C. Yan,[70] H. J. Yang,[41,e] H. X. Yang,[1] L. Yang,[42] S. L. Yang,[53] Y. X. Yang,[12] Yifan Yang,[1,53] Zhi Yang,[24] M. Ye,[1,48] M. H. Ye,[7] J. H. Yin,[1] Z. Y. You,[49] B. X. Yu,[1,48,53] C. X. Yu,[35] G. Yu,[1,53] J. S. Yu,[19,i] T. Yu,[63] C. Z. Yuan,[1,53] L. Yuan,[2] X. Q. Yuan,[37,h] Y. Yuan,[1] Z. Y. Yuan,[49] C. X. Yue,[31] A. A. Zafar,[64] X. Zeng Zeng,[6] Y. Zeng,[19,i] A. Q. Zhang,[1] B. X. Zhang,[1] Guangyi Zhang,[15] H. Zhang,[62] H. H. Zhang,[49] H. H. Zhang,[26]

112012-1

H. Y. Zhang,[1,48] J. J. Zhang,[42] J. L. Zhang,[68] J. Q. Zhang,[33] J. W. Zhang,[1,48,53] J. Y. Zhang,[1] J. Z. Zhang,[1,53] Jianyu Zhang,[1,53] Jiawei Zhang,[1,53] L. M. Zhang,[51] L. Q. Zhang,[49] Lei Zhang,[34] S. Zhang,[49] S. F. Zhang,[34] Shulei Zhang,[19,i] X. D. Zhang,[36] X. Y. Zhang,[40] Y. Zhang,[60] Y. T. Zhang,[70] Y. H. Zhang,[1,48] Yan Zhang,[62,48] Yao Zhang,[1] Z. Y. Zhang,[67] G. Zhao,[1] J. Zhao,[31] J. Y. Zhao,[1,53] J. Z. Zhao,[1,48] Lei Zhao,[62,48] Ling Zhao,[1] M. G. Zhao,[35] Q. Zhao,[1] S. J. Zhao,[70] Y. B. Zhao,[1,48] Y. X. Zhao,[24] Z. G. Zhao,[62,48] A. Zhemchugov,[28,a] B. Zheng,[63] J. P. Zheng,[1,48] Y. H. Zheng,[53] B. Zhong,[33] C. Zhong,[63] L. P. Zhou,[1,53] Q. Zhou,[1,53] X. Zhou,[67] X. K. Zhou,[53] X. R. Zhou,[62,48] X. Y. Zhou,[31] A. N. Zhu,[1,53] J. Zhu,[35] K. Zhu,[1] K. J. Zhu,[1,48,53] S. H. Zhu,[61] T. J. Zhu,[68] W. J. Zhu,[35] W. J. Zhu,[9,f] Y. C. Zhu,[62,48] Z. A. Zhu,[1,53] B. S. Zou,[1] and J. H. Zou[1]

(BESIII Collaboration)

[1]*Institute of High Energy Physics, Beijing 100049, People's Republic of China*
[2]*Beihang University, Beijing 100191, People's Republic of China*
[3]*Beijing Institute of Petrochemical Technology, Beijing 102617, People's Republic of China*
[4]*Bochum Ruhr-University, D-44780 Bochum, Germany*
[5]*Carnegie Mellon University, Pittsburgh, Pennsylvania 15213, USA*
[6]*Central China Normal University, Wuhan 430079, People's Republic of China*
[7]*China Center of Advanced Science and Technology, Beijing 100190, People's Republic of China*
[8]*COMSATS University Islamabad, Lahore Campus, Defence Road, Off Raiwind Road,*
54000 Lahore, Pakistan
[9]*Fudan University, Shanghai 200443, People's Republic of China*
[10]*G.I. Budker Institute of Nuclear Physics SB RAS (BINP), Novosibirsk 630090, Russia*
[11]*GSI Helmholtzcentre for Heavy Ion Research GmbH, D-64291 Darmstadt, Germany*
[12]*Guangxi Normal University, Guilin 541004, People's Republic of China*
[13]*Hangzhou Normal University, Hangzhou 310036, People's Republic of China*
[14]*Helmholtz Institute Mainz, Staudinger Weg 18, D-55099 Mainz, Germany*
[15]*Henan Normal University, Xinxiang 453007, People's Republic of China*
[16]*Henan University of Science and Technology, Luoyang 471003, People's Republic of China*
[17]*Huangshan College, Huangshan 245000, People's Republic of China*
[18]*Hunan Normal University, Changsha 410081, People's Republic of China*
[19]*Hunan University, Changsha 410082, People's Republic of China*
[20]*Indian Institute of Technology Madras, Chennai 600036, India*
[21]*Indiana University, Bloomington, Indiana 47405, USA*
[22a]*INFN Laboratori Nazionali di Frascati, I-00044 Frascati, Italy*
[22b]*INFN Sezione di Perugia, I-06100 Perugia, Italy*
[22c]*University of Perugia, I-06100 Perugia, Italy*
[23a]*INFN Sezione di Ferrara, I-44122 Ferrara, Italy*
[23b]*University of Ferrara, I-44122 Ferrara, Italy*
[24]*Institute of Modern Physics, Lanzhou 730000, People's Republic of China*
[25]*Institute of Physics and Technology, Peace Avenue 54B, Ulaanbaatar 13330, Mongolia*
[26]*Jilin University, Changchun 130012, People's Republic of China*
[27]*Johannes Gutenberg University of Mainz, Johann-Joachim-Becher-Weg 45, D-55099 Mainz, Germany*
[28]*Joint Institute for Nuclear Research, 141980 Dubna, Moscow region, Russia*
[29]*Justus-Liebig-Universitaet Giessen, II. Physikalisches Institut, Heinrich-Buff-Ring 16,*
D-35392 Giessen, Germany
[30]*Lanzhou University, Lanzhou 730000, People's Republic of China*
[31]*Liaoning Normal University, Dalian 116029, People's Republic of China*
[32]*Liaoning University, Shenyang 110036, People's Republic of China*
[33]*Nanjing Normal University, Nanjing 210023, People's Republic of China*
[34]*Nanjing University, Nanjing 210093, People's Republic of China*
[35]*Nankai University, Tianjin 300071, People's Republic of China*
[36]*North China Electric Power University, Beijing 102206, People's Republic of China*
[37]*Peking University, Beijing 100871, People's Republic of China*
[38]*Qufu Normal University, Qufu 273165, People's Republic of China*
[39]*Shandong Normal University, Jinan 250014, People's Republic of China*
[40]*Shandong University, Jinan 250100, People's Republic of China*
[41]*Shanghai Jiao Tong University, Shanghai 200240, People's Republic of China*
[42]*Shanxi Normal University, Linfen 041004, People's Republic of China*
[43]*Shanxi University, Taiyuan 030006, People's Republic of China*
[44]*Sichuan University, Chengdu 610064, People's Republic of China*

[45]*Soochow University, Suzhou 215006, People's Republic of China*
[46]*South China Normal University, Guangzhou 510006, People's Republic of China*
[47]*Southeast University, Nanjing 211100, People's Republic of China*
[48]*State Key Laboratory of Particle Detection and Electronics, Beijing 100049,
Hefei 230026, People's Republic of China*
[49]*Sun Yat-Sen University, Guangzhou 510275, People's Republic of China*
[50]*Suranaree University of Technology, University Avenue 111, Nakhon Ratchasima 30000, Thailand*
[51]*Tsinghua University, Beijing 100084, People's Republic of China*
[52a]*Turkish Accelerator Center Particle Factory Group, Istanbul Bilgi University,
HEP Res. Cent., 34060 Eyup, Istanbul, Turkey*
[52b]*Turkish Accelerator Center Particle Factory Group, Near East University,
Nicosia, North Cyprus, Mersin 10, Turkey*
[53]*University of Chinese Academy of Sciences, Beijing 100049, People's Republic of China*
[54]*University of Groningen, NL-9747 AA Groningen, Netherlands*
[55]*University of Hawaii, Honolulu, Hawaii 96822, USA*
[56]*University of Jinan, Jinan 250022, People's Republic of China*
[57]*University of Manchester, Oxford Road, Manchester M13 9PL, United Kingdom*
[58]*University of Minnesota, Minneapolis, Minnesota 55455, USA*
[59]*University of Muenster, Wilhelm-Klemm-Strasse 9, 48149 Muenster, Germany*
[60]*University of Oxford, Keble Road, Oxford OX13RH, United Kingdom*
[61]*University of Science and Technology Liaoning, Anshan 114051, People's Republic of China*
[62]*University of Science and Technology of China, Hefei 230026, People's Republic of China*
[63]*University of South China, Hengyang 421001, People's Republic of China*
[64]*University of the Punjab, Lahore-54590, Pakistan*
[65a]*University of Turin, I-10125 Turin, Italy*
[65b]*University of Eastern Piedmont, I-15121 Alessandria, Italy*
[65c]*INFN, I-10125 Turin, Italy*
[66]*Uppsala University, Box 516, SE-75120 Uppsala, Sweden*
[67]*Wuhan University, Wuhan 430072, People's Republic of China*
[68]*Xinyang Normal University, Xinyang 464000, People's Republic of China*
[69]*Zhejiang University, Hangzhou 310027, People's Republic of China*
[70]*Zhengzhou University, Zhengzhou 450001, People's Republic of China*

Based on 3.19 fb^{-1} of e^+e^- collision data accumulated at the center-of-mass energy 4.178 GeV with the BESIII detector operating at the BEPCII collider, the electromagnetic Dalitz decay $D^{*0} \to D^0 e^+ e^-$ is observed for the first time with a statistical significance of 13.2σ. The ratio of the branching fraction of $D^{*0} \to D^0 e^+ e^-$ to that of $D^{*0} \to D^0 \gamma$ is measured to be $(11.08 \pm 0.76 \pm 0.49) \times 10^{-3}$. By using the world average value of the branching fraction of $D^{*0} \to D^0 \gamma$, the branching fraction of $D^{*0} \to D^0 e^+ e^-$ is

[a]Also at the Moscow Institute of Physics and Technology, Moscow 141700, Russia.
[b]Also at the Novosibirsk State University, Novosibirsk, 630090, Russia.
[c]Also at the NRC "Kurchatov Institute", PNPI, 188300, Gatchina, Russia.
[d]Also at Goethe University Frankfurt, 60323 Frankfurt am Main, Germany.
[e]Also at Key Laboratory for Particle Physics, Astrophysics and Cosmology, Ministry of Education; Shanghai Key Laboratory for Particle Physics and Cosmology; Institute of Nuclear and Particle Physics, Shanghai 200240, People's Republic of China.
[f]Also at Key Laboratory of Nuclear Physics and Ion-beam Application (MOE) and Institute of Modern Physics, Fudan University, Shanghai 200443, People's Republic of China.
[g]Also at Harvard University, Department of Physics, Cambridge, Massachusetts 02138, USA.
[h]Also at State Key Laboratory of Nuclear Physics and Technology, Peking University, Beijing 100871, People's Republic of China.
[i]Also at School of Physics and Electronics, Hunan University, Changsha 410082, China.
[j]Also at Guangdong Provincial Key Laboratory of Nuclear Science, Institute of Quantum Matter, South China Normal University, Guangzhou 510006, China.
[k]Also at Frontiers Science Center for Rare Isotopes, Lanzhou University, Lanzhou 730000, People's Republic of China.
[l]Also at Lanzhou Center for Theoretical Physics, Lanzhou University, Lanzhou 730000, People's Republic of China.
[m]Present address: Istinye University, 34010 Istanbul, Turkey.

determined to be $(3.91 \pm 0.27 \pm 0.17 \pm 0.10) \times 10^{-3}$, where the first uncertainty is statistical, the second is systematic and the third is from external input of the branching fraction for $D^{*0} \to D^0 \gamma$.

I. INTRODUCTION

The conversion decays of a vector resonance (V) into a pseudoscalar meson (P) and a lepton pair, $V \to P\gamma^* \to P\ell\bar{\ell}$, provide a stringent test for theoretical models of the structure of hadrons and the interaction mechanism between photons and hadrons [1]. In these processes, the squared dilepton invariant mass corresponds to the virtual photon four-momentum transfer squared, q^2. The q^2 distribution depends on the underlying dynamical electromagnetic structure of the transition $V \to P\gamma^*$. Furthermore, through the vector-meson dominance (VMD) model [1], the virtual photon effectively couples to vector particles, such as the ρ, ω, ϕ, and even the heavier J/ψ particle. However, the off-shell effects cannot be calculated reliably [2]. Experimental measurement of the q^2 distribution is crucial to validate these calculations.

Several light meson decays with virtual photon-conversion to an e^+e^- pair, e.g., $\omega \to \pi^0 e^+ e^-$ [3], $\phi \to \pi^0 e^+ e^-$ [4], and $\phi \to \eta e^+ e^-$ [5], have been observed. The charmonium electromagnetic (EM) Dalitz decay, $\psi(3686) \to e^+ e^- \eta'$ [6], $\psi(3686) \to e^+ e^- \chi_{cJ}$ [7], and $J/\psi \to e^+ e^- \eta$ [8], have also been reported. The charm meson decay $D_s^{*+} \to D_s^+ e^+ e^-$ was observed by CLEO [9], and the ratio of the branching fractions $\frac{\mathcal{B}(D_s^{*+} \to D_s^+ e^+ e^-)}{\mathcal{B}(D_s^{*+} \to D_s^+ \gamma)}$ is measured to be $(0.72 \pm 0.18)\%$, which agrees with theoretical calculation based on the VMD model. However, there is no experimental result for the corresponding EM Dalitz decays of D^{*0} and D^{*+}. According to the VMD model, the $D_s^{*+} \to D_s^+ e^+ e^-$ decay mainly occurs via the coupling of the virtual

photon to the vector ϕ meson, while the $D^{*0} \to D^0 e^+ e^-$ decay proceeds through the coupling to the ρ or ω meson. Hence, the study of the decay $D^{*0} \to D^0 e^+ e^-$, with the diagrams depicted in Fig. 1, provides information on the form factor for the couplings $\gamma^* \to \rho$ and $\gamma^* \to \omega$. The ratio between branching fractions of $D^{*0} \to D^0 e^+ e^-$ and $D^{*0} \to D^0 \gamma$ is defined as

$$R_{ee} = \frac{\mathcal{B}(D^{*0} \to D^0 e^+ e^-)}{\mathcal{B}(D^{*0} \to D^0 \gamma)}. \tag{1}$$

Calculations using the VMD model give $R_{ee} = 0.67\%$ along with the following differential decay rate [1]:

$$\frac{dR_{ee}}{dq^2} = \frac{\alpha}{3\pi q^2} \left| \frac{f(q^2)}{f(0)} \right|^2 \left[1 - \frac{4m_e^2}{q^2} \right]^{\frac{1}{2}} \left[1 + \frac{2m_e^2}{q^2} \right]$$
$$\times \left[\left(1 + \frac{q^2}{A} \right)^2 - \frac{4m_{D^{*0}}^2 q^2}{A^2} \right]^{\frac{3}{2}}. \tag{2}$$

Here, α is the fine structure constant, $A = m_{D^{*0}}^2 - m_{D^0}^2$, $f(q^2)$ is the transition form factor for D^{*0} to D^0, m_e is the mass of electron and $m_{D^{*0}}$ (m_{D^0}) is the mass of D^{*0} (D^0). The form-factor ratio $\frac{f(q^2)}{f(0)}$ is equal to $(1 - \frac{q^2}{m_\rho^2})^{-1}$, where m_ρ is the ρ resonance mass.

In this paper, the EM Dalitz decay $D^{*0} \to D^0 e^+ e^-$ is studied and R_{ee} is measured using 3.19 fb^{-1} of e^+e^- collision data collected with the BESIII detector at the center-of-mass energy $\sqrt{s} = 4.178$ GeV. To control background contributions, the candidates for both $D^{*0} \to D^0 e^+ e^-$ and $D^{*0} \to D^0 \gamma$ are reconstructed with $e^+ e^- \to D^{*0} \bar{D}^{*0}$ events. The single tag method is used, so that only D^{*0} ($\bar{D}^{*0}$) is reconstructed and the $\bar{D}^{*0}(D^{*0})$ on the recoiling side is not detected. The inclusion of charge-conjugate states is implied throughout this paper.

(a)

(b)

FIG. 1. Diagrams of the decay $D^{*0} \to D^0 e^+ e^-$. The symbol V^* indicates the virtual ρ, ω, ϕ, or J/ψ meson.

II. DESCRIPTION OF THE BEPCII AND THE BESIII DETECTOR

The BESIII detector [10] records symmetric e^+e^- collisions provided by the BEPCII storage ring [11], which operates in the center-of-mass energy range from 2.0–4.96 GeV. BESIII has collected large data samples in this energy region [12]. The cylindrical core of the BESIII detector covers 93% of the full solid angle and consists of a helium-based multilayer drift chamber (MDC), a plastic scintillator and multi-gap resistive plate chamber time-of-flight system (TOF), and a CsI(Tl) electromagnetic
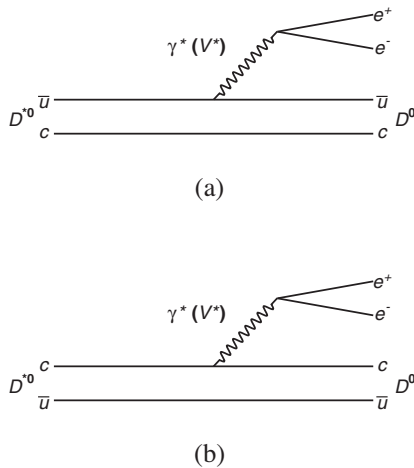
calorimeter (EMC), which are all enclosed in a super-conducting solenoidal magnet providing a 1.0 T magnetic field. The solenoid is supported by an octagonal flux-return yoke with resistive plate counter muon identification modules interleaved with steel. The charged-particle momentum resolution at 1 GeV/c is 0.5%, and the dE/dx resolution is 6% for electrons from Bhabha scattering. The EMC measures photon energies with a resolution of 2.5% (5%) at 1 GeV in the barrel (end cap) region. The time resolution in the TOF barrel region is 68 ps, while that in the end cap region is 60 ps [13].

III. MONTE CARLO SIMULATION

Simulated data samples produced with a GEANT4-based [14] Monte Carlo (MC) package, which includes the geometric description of the BESIII detector and the detector response, are used to determine detection efficiencies and to estimate backgrounds. The simulation models the beam energy spread and initial state radiation (ISR) in the e^+e^- annihilations with the generator KKMC [15]. The inclusive MC sample includes the production of open charm processes, the ISR production of vector charmonium(-like) states, and the continuum processes incorporated in KKMC [15]. The known decay modes are modeled with EVTGEN [16] using branching fractions taken from the Particle Data Group [17], and the remaining unknown charmonium decays are modeled with LUNDCHARM [18]. Final state radiation (FSR) from charged final state particles is incorporated using PHOTOS [19].

The MC events of the signal process $e^+e^- \to D^{*0}\bar{D}^{*0}$, $D^{*0} \to D^0 e^+ e^-$ are generated according to the VMD model. Following Ref. [20], the decay $D^{*0} \to D^0 e^+ e^-$ is described as

$$\frac{d\Gamma}{dq^2 d\cos\theta_e} \propto \frac{|f(q^2)|^2}{q^2}\left(1 - \frac{4m_e^2}{q^2}\right)^{\frac{1}{2}}$$
$$\times [(m_{D^{*0}}^2 - m_{D^0}^2 + q^2)^2 - 4m_{D^{*0}}^2 q^2]^{\frac{3}{2}}$$
$$\times \left[\left(1 + \frac{4m_e^2}{q^2}\right) + \left(1 - \frac{4m_e^2}{q^2}\right)\cos^2\theta_e\right], \quad (3)$$

where θ_e is the helicity angle of the electron pair system. The MC samples of the reference process $D^{*0} \to D^0\gamma$ are generated with the KKMC.

IV. EVENT SELECTION

To reconstruct the signal and reference processes, D^0 candidates are selected via three decay modes $D^0 \to K^-\pi^+$, $K^-\pi^+\pi^0$, and $K^-\pi^+\pi^-\pi^+$. For each charged track candidate, the polar angle θ in the MDC is required to be in the range $|\cos\theta| < 0.93$, and the distance of closest approach to the interaction point is required to be less than 10 cm

along the beam direction and less than 1 cm in the plane perpendicular to the beam. The dE/dx recorded by the MDC and the time-of-flight information measured by the TOF are combined to calculate particle identification (PID) probability for the pion ($\mathcal{P}_\pi$) and kaon ($\mathcal{P}_K$) hypotheses. Pion candidates are selected by requiring $\mathcal{P}_\pi > 0$ and $\mathcal{P}_\pi > \mathcal{P}_K$, and kaon candidates are required to satisfy $\mathcal{P}_K > 0$ and $\mathcal{P}_K > \mathcal{P}_\pi$. Photon candidates are reconstructed with isolated clusters in the EMC in the region $|\cos\theta| \leq 0.80$ (barrel) or $0.86 \leq |\cos\theta| \leq 0.92$ (end cap). The deposited energy of the cluster is required to be larger than 25 (50) MeV in the barrel (end cap) region, and the angle between the photon candidate and any charged track is larger than 10°. All $\gamma\gamma$ combinations are considered as candidate π^0 mesons, and the reconstructed mass $M_{\gamma\gamma}$ is required to satisfy $0.115 < M_{\gamma\gamma} < 0.150$ GeV/c^2. A kinematic fit is performed to constrain the $\gamma\gamma$ invariant mass to the nominal π^0 mass taken from the PDG [17], and candidates with the fit quality $\chi^2 < 200$ are retained. The $K^-\pi^+$, $K^-\pi^+\pi^0$, and $K^-\pi^+\pi^-\pi^+$ combinations are required to be within the mass windows $1.85 < M_{K^-\pi^+} < 1.88$ GeV/c^2, $1.84 < M_{K^-\pi^+\pi^0} < 1.89$ GeV/c^2 and $1.85 < M_{K^-\pi^+\pi^-\pi^+} < 1.88$ GeV/c^2, respectively. For each decay mode, all possible combinations are kept for further analysis.

For the $D^{*0} \to D^0 e^+ e^-$ decay, the electron and positron candidates are identified among the remaining charged tracks with the dE/dx information measured by the MDC. The probability criteria of $\mathcal{P}_e > 0$, $\mathcal{P}_e > \mathcal{P}_\pi$, and $\mathcal{P}_e > \mathcal{P}_K$ are applied. The energy difference ΔE is defined as $\Delta E = E_{D^{*0}} - E_{\text{beam}}$, where $E_{D^{*0}}$ is the reconstructed energy of D^{*0} candidates in the rest frame of the e^+e^- initial beams and E_{beam} is the beam energy; $|\Delta E| < 0.03$ GeV is required to reduce background contributions. If there are multiple candidates (13% of the selected events) in an event, only the one with the minimum $|\Delta E|$ is accepted. Similarly, for the $D^{*0} \to D^0\gamma$ candidates, if there are multiple combinations (32% of the selected events) in an event, only the candidate with the minimum $|\Delta E|$ is kept and $|\Delta E| < 0.03$ GeV is required to reduce backgrounds. To separate D^{*0} candidates produced from $e^+e^- \to D^{*0}\bar{D}^{*0}$ from backgrounds, the beam-constrained mass M_{BC} is defined as $M_{\text{BC}}^2 = E_{\text{beam}}^2 - p_{D^{*0}}^2$, where $p_{D^{*0}}$ is the measured total momentum of D^{*0} candidates in the rest frame of initial e^+e^- beams. In addition, a veto for dielectrons from photon conversion is applied to suppress background from $D^{*0} \to D^0\gamma$, where the dielectron comes from the transition photon interacting with the materials in the beam pipe and the MDC inner wall. The variable of R_{xy} which represents the distance between beam interaction point and vertex of photon-conversion in xy plane [21] is calculated. Figure 2(a) shows the R_{xy} distribution of the $D^{*0} \to D^0 e^+ e^-$ candidates, where two clear peaks
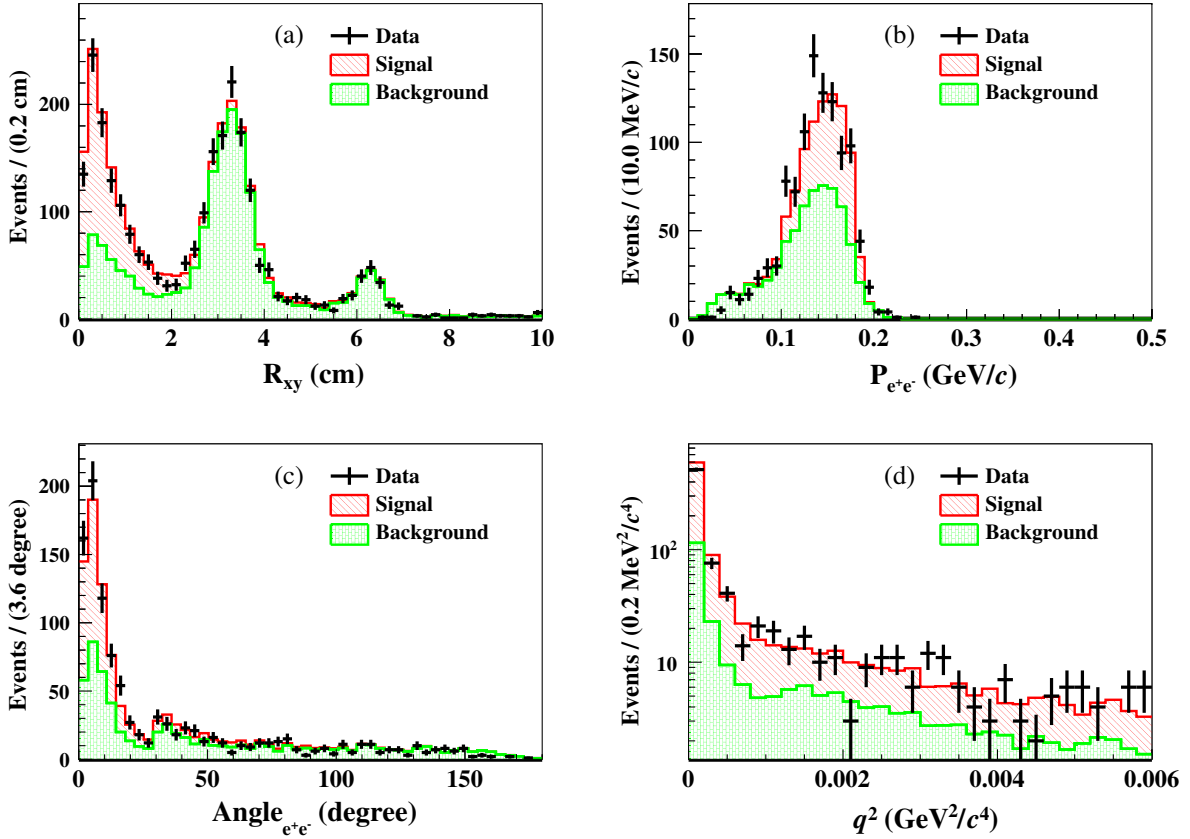
FIG. 2.   The distributions of (a) R_{xy}, (b) the momentum of the e^+e^- pair, (c) the angle between e^+ and e^- in the laboratory frame and (d) the virtual photon four-momentum transfer square (q^2) of the candidates for $D^{*0} \to D^0 e^+ e^-$. The points with error bars are data. The brick-filled green histograms indicate the scaled backgrounds derived from inclusive MC samples. The slash-filled red histograms label the normalized signal $D^{*0} \to D^0 e^+ e^-$ contributions, extracted from the signal MC samples. For all distributions, the three D^0 decay modes are combined and M_{BC} is required to be in the region $(2.00, 2.02)$ GeV/c^2. The distributions of (b), (c) and (d) show events passing the $R_{xy} < 2.0$ cm requirement.
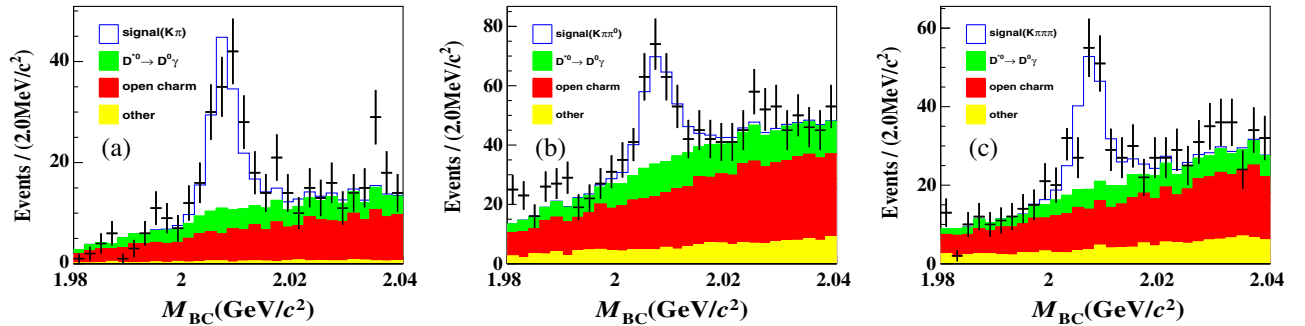
FIG. 3.   The comparison between data and MC components for $D^{*0} \to D^0 e^+ e^-$ process, where plot (a) is for $D^0 \to K^- \pi^+$ mode, plot (b) for $D^0 \to K^- \pi^+ \pi^0$ mode and plot (c) for $D^0 \to K^- \pi^+ \pi^- \pi^+$ mode. Black dots with error bars are data, the blue lines are signal processes. The shaded histograms are the background processes for $D^{*0} \to D^0 \gamma$ (green), open charm (red) and other (yellow) processes, respectively.

corresponding to the beam pipe position (3 cm) and the MDC inner wall (6 cm) are observed. An additional requirement $R_{xy} < 2.0$ cm removes the photon-conversion events. Figures 2(b), 2(c), and 2(d) show the distributions of the

momentum of the e^+e^- pair, the opening angle between e^+ and e^-, and the q^2 of the e^+e^- candidates for the $D^{*0} \to D^0 e^+ e^-$, respectively. Good agreement between data and MC simulation is seen in Fig. 3.

V. DETERMINATION OF THE BRANCHING FRACTION

In the data sample, the observed number of signal events is expressed as

$$N_{\text{sig}} = 2 \cdot N_{D^{*0}\bar{D}^{*0}} \cdot \mathcal{B}(D^{*0} \to D^0 e^+ e^-) \cdot \mathcal{B}_{\text{int}} \cdot \varepsilon_{\text{sig}}, \quad (4)$$

and the observed number of the reference process as

$$N_{\text{ref}} = 2 \cdot N_{D^{*0}\bar{D}^{*0}} \cdot \mathcal{B}(D^{*0} \to D^0 \gamma) \cdot \mathcal{B}_{\text{int}} \cdot \varepsilon_{\text{ref}}. \quad (5)$$

Here, $N_{D^{*0}\bar{D}^{*0}}$ is the total number of $D^{*0}\bar{D}^{*0}$ pairs in data, ε_{sig} and ε_{ref} denote the detection efficiencies of the signal and reference processes, respectively, and $\mathcal{B}_{\text{int}}$ stands for the branching fractions for the three D^0 decay modes and secondary decay of the π^0 meson. For the signal process, the efficiency ε_{sig} has been corrected to account for differences of the photon conversion, tracking and PID efficiencies between data and MC simulation (see discussion of systematic uncertainties below). Thus, the ratio R_{ee} for each decay mode is given as

$$R_{ee} = \frac{\mathcal{B}(D^{*0} \to D^0 e^+ e^-)}{\mathcal{B}(D^{*0} \to D^0 \gamma)} = \frac{N_{\text{sig}} \cdot \epsilon_{\text{ref}}}{N_{\text{ref}} \cdot \epsilon_{\text{sig}}}. \quad (6)$$

The individual yields of the signal and reference processes are obtained by simultaneous fits to the M_{BC} distributions. The M_{BC} distributions of the accepted candidates for both signal and reference channels are shown in Fig. 4. In the fits, the signal shapes are obtained from the corresponding simulated shapes convolving with Gaussian functions to compensate the resolution difference between data and MC simulation. A common R_{ee} is used for all three tag modes in the simultaneous fit, after the relevant efficiencies and branching fractions for each D^0 mode are taken into account. Note that peaking contributions from the corresponding doubly Cabibbo suppressed modes $\bar{D}^0 \to K^-\pi^+$, $K^-\pi^+\pi^0$, and $K^-\pi^+\pi^-\pi^+$ cancel out in calculating R_{ee}. Background studies indicate no peaking structures in the fit range, as illustrated in Fig. 4. Hence, a second-order polynomial function is used to describe the combinatorial backgrounds. The final fit results are also shown in Fig. 4, and the numerical results of the efficiencies and yields are listed in Table I. The ratio R_{ee} is determined to be $(11.08 \pm 0.76) \times 10^{-3}$, where the uncertainty is statistical. The statistical significance is estimated to be 13.2σ. The R_{ee} values obtained separately in the three D^0 tag modes are consistent. By using the world average value of the branching fraction of $D^{*0} \to D^0\gamma$, the branching fraction of $D^{*0} \to D^0 e^+ e^-$ is calculated to be $(3.91 \pm 0.27) \times 10^{-3}$.

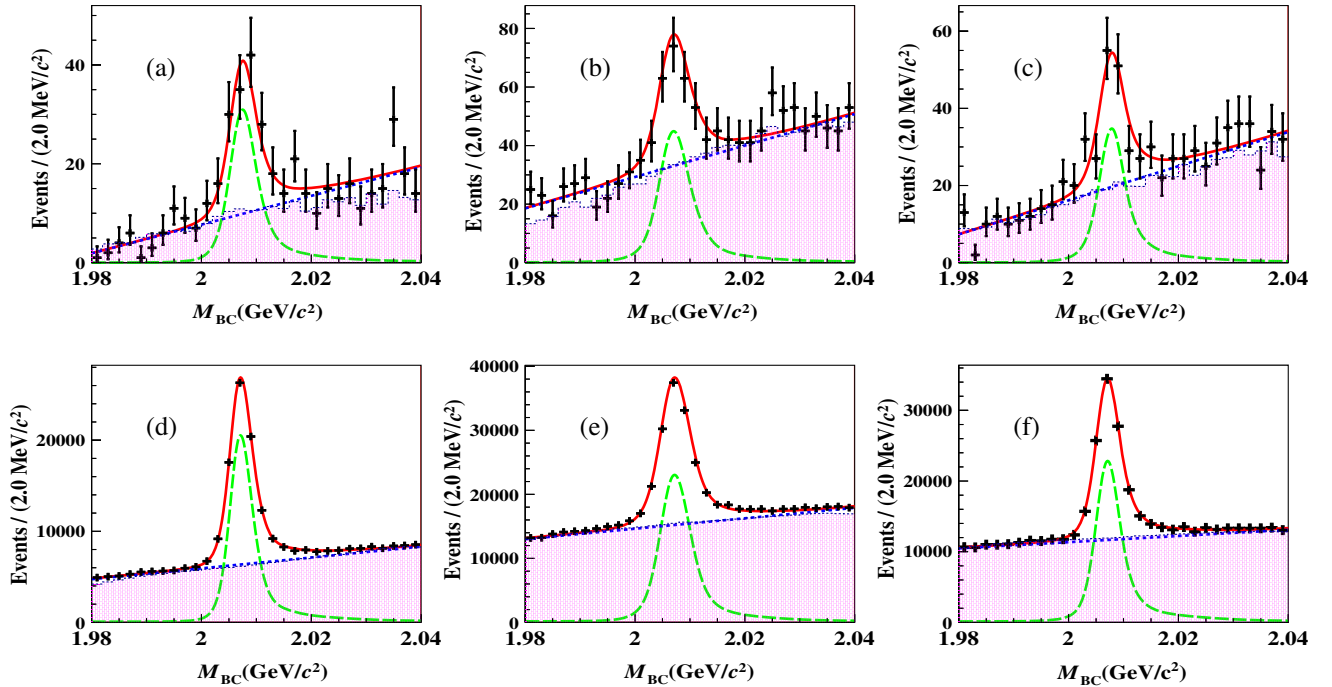FIG. 4. Fits to the M_{BC} distributions of the candidates for $D^{*0} \to D^0 e^+ e^-$ (top) and $D^{*0} \to D^0\gamma$ (bottom), plots (a) and (d) are reconstructed using $D^0 \to K^-\pi^+$ mode, plots (b) and (e) are reconstructed using $D^0 \to K^-\pi^+\pi^0$ mode. Plots (c) and (f) are reconstructed using $D^0 \to K^-\pi^+\pi^-\pi^+$ mode. Black dots with error bars are data, the solid red lines are total fits, the long-dashed green lines are signals and the dotted blue lines are smooth backgrounds. The shaded areas represent the MC-predicted backgrounds.

TABLE I.   Yields and efficiencies of the three D^0 tag decay modes and the obtained branching fractions. For the obtained branching fractions, the first uncertainties are statistical and the second systematic, while the uncertainties are statistical only for the other numbers. The third systematic uncertainty is quoted from the uncertainty of $D^{*0} \to D^0 \gamma$ in PDG.

	$D^0 \to K^- \pi^+$	$D^0 \to K^- \pi^+ \pi^0$	$D^0 \to K^- \pi^+ \pi^- \pi^+$
ϵ_{ref} (%)	35.82 ± 0.28	14.81 ± 0.20	19.11 ± 0.15
N_{ref}	66484 ± 223	97471 ± 327	74196 ± 249
ϵ_{sig} (%)	5.61 ± 0.04	2.58 ± 0.03	3.09 ± 0.03
N_{sig}	111.3 ± 7.6	181.5 ± 12.4	128.1 ± 8.7
R_{ee}		$(11.08 \pm 0.76 \pm 0.49) \times 10^{-3}$	
$\mathcal{B}(D^{*0} \to D^0 e^+ e^-)$		$(3.91 \pm 0.27 \pm 0.17 \pm 0.10) \times 10^{-3}$	

VI. SYSTEMATIC UNCERTAINTY

The main sources of systematic uncertainties are summarized in Table II and discussed in detail next. Systematic uncertainties in D^0 reconstruction are canceled in the ratio R_{ee}.

To study the efficiencies of the tracking and PID of low-momentum $e^\pm$, a control sample of $e^+ e^- \to \gamma e^+ e^-$ is selected. Due to relatively large efficiency differences, a reweighting procedure according to the two-dimensional kinematic distribution in transverse momentum and $\cos\theta$ is implemented to reweight the MC-determined efficiency of $D^{*0} \to D^0 e^+ e^-$. The overall correction factor is estimated to be $(108.5 \pm 2.9)\%$ for $e^+ e^-$ pair. For $e^\pm$ PID, the same control sample and reweighting procedure are used. The corresponding overall correction factor is estimated to be $(94.1 \pm 1.4)\%$. After correcting the signal efficiencies to data, the uncertainty on the correction factor is assigned as the systematic uncertainties.

In the reference mode $D^{*0} \to D^0 \gamma$, the uncertainty in the reconstruction efficiency of photon is assigned to be 1.0% based on the studies with a control sample of $J/\psi \to \rho^0 \pi^0$ events [22].

In the nominal analysis, the PDG value of m_ρ is used in the form factor of $D^{*0} \to D^0 e^+ e^-$ in the signal generator. In order to assign an uncertainty, we replace m_ρ with m_ω in the form factor in Eq. (2). The resultant change on the efficiency, 1.1%, is taken as the systematic uncertainty.

The signal efficiency loss due to vetoing photon conversions ($R_{xy} < 2.0$ cm) is studied with a control sample of $e^+ e^- \to \gamma J/\psi$, $J/\psi \to \pi^0 \pi^+ \pi^-$ with π^0 decaying to $\gamma e^+ e^-$ final state. The veto efficiency is found to be lower than that determined in MC simulation by a factor $(96.4 \pm 1.0)\%$. After correcting the signal efficiencies to data, we assign 1.0% as the corresponding systematic uncertainty.

The efficiencies of the ΔE requirements are estimated by correcting the variable ΔE in the MC sample according to the observed resolution difference between data and MC simulation. The change of the obtained efficiencies of the corrected signal MC samples from the nominal efficiencies is taken as systematic uncertainty. For the fits to the M_{BC} distributions, the signal shapes are varied from the MC-derived shape convolved with a single-Gaussian function to one using MC simulation convolved with a double-Gaussian function, while the background shape is varied from a second-order polynomial function to a linear function. The resultant changes on the final result are adopted as systematic uncertainties.

VII. SUMMARY

Based on 3.19 fb^{-1} of $e^+ e^-$ collision data collected at $\sqrt{s} = 4.178$ GeV with the BESIII detector, the EM Dalitz decay $D^{*0} \to D^0 e^+ e^-$ is observed for the first time. The branching fraction of this decay relative to that of $D^{*0} \to D^0 \gamma$ is measured to be $(11.08 \pm 0.76 \pm 0.49) \times 10^{-3}$. This result deviates from the ratio of 0.67% according to Eq. (2) with 3.5σ. Using the world average $\mathcal{B}(D^{*0} \to D^0 \gamma) = (35.3 \pm 0.9)\%$ [17], we determine $\mathcal{B}(D^{*0} \to D^0 e^+ e^-) = (3.91 \pm 0.27 \pm 0.17 \pm 0.10) \times 10^{-3}$, where the first uncertainty is statistical, the second is systematic and the third is from the uncertainty of the input $\mathcal{B}(D^{*0} \to D^0 \gamma)$. The obtained distribution of virtual photon four-momentum transfer square is compatible with the model prediction in Eq. (2), as shown in Fig. 2(d). However, the statistics for now is still low for meaningful measurements of the q^2-dependent form factor. Better precisions can be achieved

TABLE II.   Systematic uncertainties in measuring R_{ee}.

Source	Uncertainty (%)
$e^\pm$ tracking	2.9
$e^\pm$ PID	1.4
Photon detection	1.0
Signal Generator	1.1
Photon conversion rejection	1.0
ΔE requirement	1.1
Signal shape	1.1
Background shape	1.7
Total	4.4

with more data taken at BESIII in the future [12], which could be used for more physics goals, such as searching for the light vector boson $X17$ decaying into the $e^+ e^-$ pairs [23].

[1] L. G. Landsberg, Phys. Rep. **128**, 301 (1985).
[2] J. J. Wu, T. S. H. Lee, and B. S. Zou, Phys. Rev. C **100**, 035206 (2019).
[3] M. N. Achasov, K. I. Beloborodov, A. V. Berdyugin, A. G. Bogdanchikov, A. D. Bukin, D. A. Bukin, A. V. Vasilev, V. B. Golubev, T. V. Dimova, V. P. Druzhinin et al., J. Exp. Theor. Phys. **107**, 61 (2008).
[4] A. Anastasi et al. (KLOE-2 Collaboration), Phys. Lett. B **757**, 362 (2016).
[5] D. Babusci et al. (KLOE-2 Collaboration), Phys. Lett. B **742**, 1 (2015).
[6] M. Ablikim et al. (BESIII Collaboration), Phys. Lett. B **783**, 452 (2018).
[7] M. Ablikim et al. (BESIII Collaboration), Phys. Rev. Lett. **118**, 221802 (2017).
[8] M. Ablikim et al. (BESIII Collaboration), Phys. Rev. D **99**, 012006 (2019).
[9] D. Cronin-Hennessy et al. (CLEO Collaboration), Phys. Rev. D **86**, 072005 (2012).
[10] M. Ablikim et al. (BESIII Collaboration), Nucl. Instrum. Methods Phys. Res., Sect. A **614**, 345 (2010).
[11] C. H. Yu et al., Proceedings of IPAC2016, Busan, Korea (JACoW, Geneva, Switzerland, 2016).
[12] M. Ablikim et al. (BESIII Collaboration), Chin. Phys. C **44**, 040001 (2020).
[13] X. Li et al., Radiat. Detect. Technol. Methods **1**, 13 (2017); Y. X. Guo et al., Radiat. Detect. Technol. Methods **1**, 15 (2017); P. Cao et al., Nucl. Instrum. Methods Phys. Res., Sect. A **953**, 163053 (2020).
[14] S. Agostinelli et al. (GEANT4 Collaboration), Nucl. Instrum. Methods Phys. Res., Sect. A **506**, 250 (2003).
[15] S. Jadach, B. F. L. Ward, and Z. Was, Phys. Rev. D **63**, 113009 (2001); Comput. Phys. Commun. **130**, 260 (2000).
[16] D. J. Lange, Nucl. Instrum. Methods Phys. Res., Sect. A **462**, 152 (2001); R. G. Ping, Chin. Phys. C **32**, 599 (2008).
[17] P. A. Zyla et al. (Particle Data Group), Prog. Theor. Exp. Phys. **2020**, 083C01 (2020).
[18] J. C. Chen, G. S. Huang, X. R. Qi, D. H. Zhang, and Y. S. Zhu, Phys. Rev. D **62**, 034003 (2000); R. L. Yang, R. G. Ping, and H. Chen, Chin. Phys. Lett. **31**, 061301 (2014).
[19] E. Richter-Was, Phys. Lett. B **303**, 163 (1993).
[20] Y. Tan, Z. Zhang, and X. Zhou, arXiv:2111.04932.
[21] Z. R. Xu and K. L. He, Chin. Phys. C **36**, 742 (2012).
[22] M. Ablikim et al. (BESIII Collaboration), Phys. Rev. D **81**, 052005 (2010).
[23] G. L. Castro and N. Quintero, Phys. Rev. D **103**, 093002 (2021).